THERMAL LOAD IN A MEDIUM-SIZED EUROPEAN CITY USING THE EXAMPLE OF AACHEN, GERMANY

Mareike Buttstädt and Christoph Schneider

Summary: In this paper we focus on air temperature and its distribution within a medium-sized European city (Aachen) to identify those areas where high levels of thermal load are likely to be observed. The temperatures for the whole city area are examined by means of a GIS-based model. This approach based on mobile measurements demonstrates the distribution of air temperature differences in relation to a reference station and allows for a detailed analysis of the influencing factors of urban structure and land use. Despite the fact that air temperature distribution in Aachen is largely determined by terrain, the influences of land use and urban structures are apparent in the model results. The evaluation of afternoon and evening air temperature data for the summer half-year (April–September) show that the importance of factors contributing to thermal load varies in the course of the day. During daytime the highest air temperature arises in industrial areas with a high degree of surface sealing. However, during the evening inner-city residential quarters with a dense building structure show the highest thermal load. Forest and green spaces also determine the specific air temperature patterns but their impact varies in the course of the day and with the size of neighborhood used for correlation statistics. The spatial structure of the modeled temperature distribution is in accordance with the spatial structure of the surface radiant temperatures from a thermal image over wide areas of Aachen. Deviations are obvious for buildings whose roof materials cause surface temperatures that differ significantly from air temperatures modeled for the 2 m level. Furthermore, the comparison makes obvious the limits of the model: the effects of cold air drainage flows and wind directions cannot be assessed. However, this is not considerably detrimental to the results.

Zusammenfassung: Vorliegender Beitrag befasst sich mit der Temperaturverteilung innerhalb der Stadt Aachen und der Identifizierung potenziell thermischer Belastungsgebiete. Mittels eines GIS-gestützten Modells, das auf mobilen Lufttemperaturmessungen basiert, werden Temperaturdifferenzen zu einer Referenzstation dargestellt und Einflussfaktoren innerhalb der urbanen Struktur ausfindig gemacht. Obwohl die Temperaturverteilung in der Stadt u.a. stark von der Topographie abhängig ist, spiegelt sich auch der Einfluss der Landnutzung und der städtischen Oberflächenstrukturen in den Ergebnissen wider. Die Analyse mittäglicher und abendlicher Lufttemperaturen für das Sommerhalbjahr (April–September) zeigt, dass der Einfluss dieser Faktoren in Abhängigkeit der Tageszeit variiert. Während Industriegebiete mit einem hohen Versiegelungsgrad die höchsten Lufttemperaturen am Tag aufweisen, begünstigen dicht bebaute Gebiete in der Innenstadt vor allem abends und nachts hohe Lufttemperaturen. Wald und Grünflächen bestimmen ebenfalls das Temperaturmuster in der Stadt. Dieses ist neben der betrachteten Tageszeit auch abhängig vom gewählten Einzugsgebiet der Korrelationsfaktoren. Der Vergleich mit Oberflächenstrahlungstemperaturen zeigt eine gute Übereinstimmung der räumlichen Temperaturmuster in weiten Teilen des Stadtgebietes. Positive Abweichungen liegen vor allem an Gebäuden vor, deren Dachmaterialien Oberflächentemperaturen generieren, die stark von den Lufttemperaturen im 2 m-Niveau abweichen. Der Vergleich zeigt zudem Grenzen des Modells–auch wenn diese die Ergebnisse nicht wesentlich verschlechtern–auf, die in der Vernachlässigung von Kaltluftströmen und der Windrichtung zu sehen sind.

Keywords: Urban climate, GIS, North Rhine-Westphalia, urban heat island

1 Introduction

Today, more than half of the world's population already lives in cities and the proportion of urban residents is expected to further increase in the future. In Germany, almost 74% of the population are urban dwellers, who are frequently exposed to environmental impacts such as air pollutants, noise and thermal load.

Thermal load in agglomerations is intensified by anthropogenic conversion of natural soils into impervious surfaces such as concrete and asphalt leading to an altered radiation balance (Oke 1980; Lee 1984; Kuttler 2001). Energy gains and losses are changed by building configurations and their thermal properties, waste heat radiation and potentiality for evaporation. All of these factors affect the temperature distribution in urban areas and

may contribute to elevated temperatures in cities compared to their surrounding environment, i.e. to the evolution of an urban heat island (UHI) (Oke 2001; Arnfield 2003; Unger 2004). Especially burdened are those city districts that are characterized by sealed surfaces, dense building structures, sparse vegetation and anthropogenic heat release. Within these built-up areas, roofing and paving often account for those surfaces whose materials–such as bitumen, asphalt or concrete–possess low albedo values so that a large proportion of the incoming solar radiation is absorbed (~80%) (Oke 2001). In many cities the UHI is most pronounced between the late evening and the early morning (Tayanç and Toros 1997; Klysik and Fortuniak 1999; Montávez et al. 2000; Unger et al. 2001; Parlow 2003; Heisler and Brazel 2010) because the construction materials, which have higher heat capacities than surface types in rural settings (e.g. soils), trigger a gradually release of heat that has been effectively stored during the day (Oke 1982). This, in turn, prevents cooling of the ambient air and, hence, amplifies the canopy UHI (see Oke (2001) for a definition of a canopy UHI). Another important factor influencing thermal conditions in urban areas other than in natural landscapes is the absence of green spaces. Sparse vegetation reduces evaporative cooling and thus also compounds the UHI (Saito et al. 1990/91; Bruse 2003).

Beside research on canopy UHIs, the surface UHIs have been investigated in many studies. The objectives are to determine the amount of sensible and latent heat fluxes that can be ascribed to different surface materials and to assess the relationship between surface temperatures and air temperatures. Surface temperatures are recorded using satellite (e.g. Eliasson 1992; Nichol et al. 2009) or aircraft-borne (e.g. Pease et al. 1976; Bärring and Mattsson 1985) infrared thermal scanners. Unlike satellite-derived data, which usually have a coarse spatial resolution (more than 50 m), data acquired from aircraft provide a higher resolution (less than 10 m) and are more adequate for micro-scale urban climatology (Lo et al. 1997).

Thermal load is an environmental stressor that may negatively affect human health or even increase mortality rates (Dobler and Jendritzky 2001; Rosenzweig et al. 2005). Since predominantly elderly people are affected (Huynen et al. 2001; Havenith 2005; Harlan et al. 2006; Gabriel and Endlicher 2011), it is necessary to take into consideration the demographic changes that lead to an ageing society in Europe (Brücker 2005;

Grundy 2006; EUROPEAN COMMISSION 2010). In Aachen, the proportion of residents aged 50 or older is expected to rapidly rise from 37% (2010) to 45% by 2020 (STADT AACHEN 2009). The most vulnerable people in the group of elderly are those who live in cities because agglomerations are characterized by temperature modifications due to the pronounced effects of human activities (Landsberg 1970; Oke 1997).

To record air temperature variations at a height above the surface that is relevant for humans, data are commonly collected at 2 m above the ground (Svensson et al. 2002) using fixed weather stations complemented by mobile measurements. Various urban climatological studies revert to data from mobile measurements made by using trams (Yamashita 1996), automobiles (Straka et al. 1996; Montávez et al. 2000; Unger et al. 2001; Bottyán and Unger 2003; Unger 2004) or bicycles (Heusinkveld et al. 2010). During mobile measurements only a limited number of meteorological parameters are measured. Therefore, approximations are frequently applied to quantify missing values (Mirzaei and Haghighat 2010). However, one main advantage of using air temperature data collected by mobile carriers instead of data recorded at fixed stations is the much better spatial representation of the variability of urban canopy layer conditions. Observations at fixed stations only depict air temperature conditions in the immediate vicinity of the station. For the city of Aachen (Germany) urban climate has mainly been investigated based on data recorded at fixed stations. A climate expertise for the city was carried out using thermal imagery (Havlik and Ketzler 2000). Until now, a statistical model for spatial patterns of air temperature has not been made using a dense network of mobile measurements.

This study aims to model the spatial temperature distribution as a pointer to the thermal load in cities and to identify the causative land use factors. The data base consists of a large quantity of air temperature data from high resolution mobile measurements along public bus routes and of detailed land use data for the city of Aachen. A statistical approach incorporating data on urban land use and topography can also be declared by Hjort et al. (2011) as a "cost efficient" and "satisfactory" method to predict temperature on a regional scale. The model output is further compared to thermal imagery in order to examine similarities and differences between modeled air temperature data and surface radiant temperatures.

2   Study area

The city of Aachen is situated in western Germany near the borders to Belgium and the Netherlands. Its basin location with differences in terrain height of up to 285 m (Fig. 1, left) causes significant local climate phenomena in the urban area. A specific setting of Aachen is the radial position of small valleys reaching into the inner city and facilitating the penetration of cold air drainage flows into the city centre during nighttime. With a size of approximately 160 km² and 245,000 residents, Aachen can be described as a medium-sized city that is representative for Central Europe in terms of spatial dimension and population size. At present, the most vulnerable population group of elderly people lives mainly in the south of Aachen (STADT AACHEN 2009). In the future, the proportion of elderly within the inner city is expected to rise as the proportion of those who migrate into the city core is assumed to increase in age (BBSR

2011). The inner-city district is characterized by a high density of buildings. A high degree of surface sealing can also be found in industrial and commercial areas to the north and northeast of the inner-city district. While the southern parts of Aachen are distinguished by open spaces, forests, and less dense building structures, the northern and north-western districts are mostly agricultural land (Fig. 1, right).

3   Data collection and handling

3.1 Measurement design

In this study, data from highly resolved air temperature measurements using public transport buses were examined. The vehicles were equipped with GPS devices (Winner fly i-gotU) and temperature loggers (Hobo Pro v2), which were installed in a radiation-shielded instrument mounted at the front of each bus
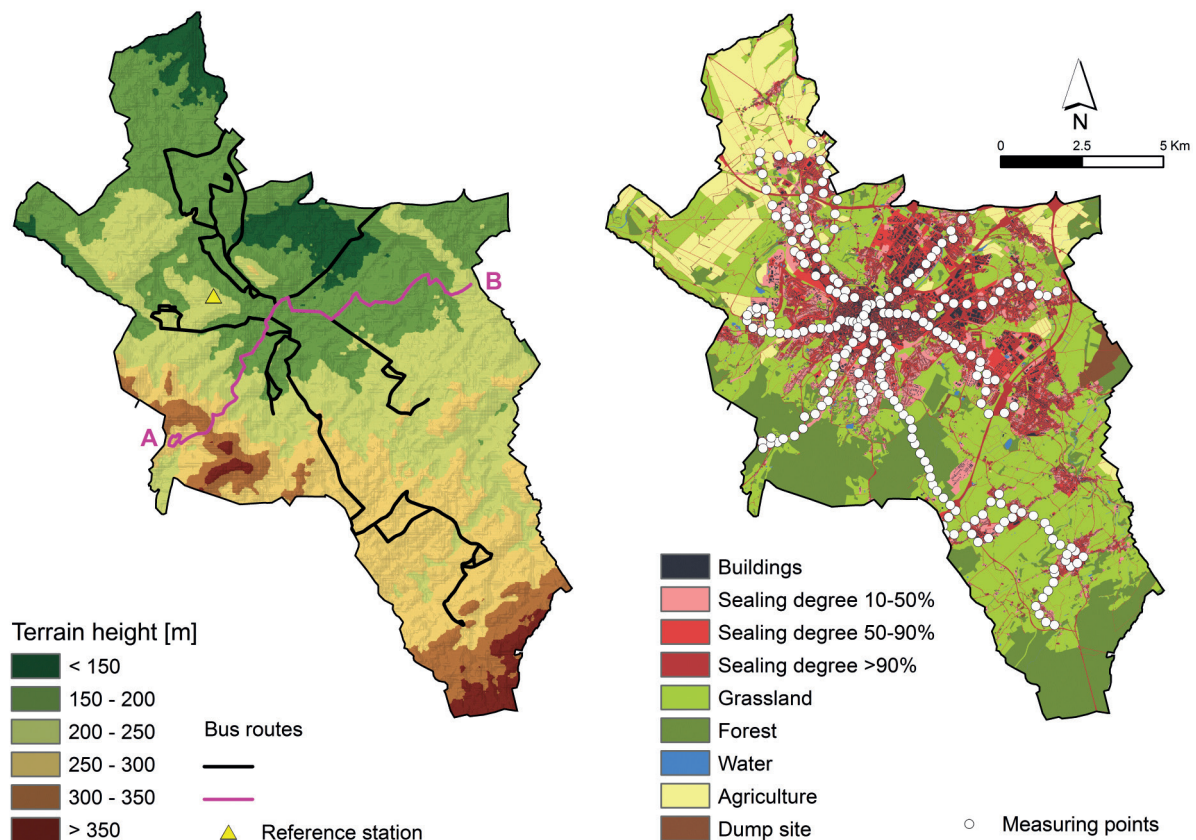

Fig. 1: Left: Digital elevation model (NASA et al. 2009) and bus routes in the study area (city of Aachen). The purple transect from the starting point A to the end point B has been chosen for a detailed analysis of the relationship between air temperature and land uses (see chapter 5). Right: Land use classification and measuring points along the bus routes

above the driver's seat. Four routes were selected, each traversed by one bus from the early morning until the late evening. The temperature data were recorded simultaneously along the four traverses at intervals of 5 seconds with an accuracy of ±0.2 °C. GPS data were stored every 15 seconds and lowered to an interval of 10 seconds when the driving speed exceeded 13.9 m/s (50 km/h). With a scheduled time-table and fixed routes, the main advantage of this approach is the regularly operating bus routes that cover different urban settings. The recorded data were assigned to predefined points along the measurement routes (256 points in total) with an average distance of about 250 m to each other. The measurement approach is documented in more detail by Buttstädt et al. (2011). Data collected on 44 days between March 2010 and June 2011 were available. Of this data, only those days with precipitation less than 0.5 mm were used in order to eliminate errors from water adhering to the temperature sensor. Furthermore, data collected at a driving speed of less than 5 m/s (18 km/h) were not considered in order to ensure sufficient sensor ventilation.

For the spatial analysis with focus on thermal load, only days of the summer half-year (April–September) with a diurnal temperature amplitude of at least 7 K were taken into consideration for data evaluation. The threshold of 7 K was chosen to ensure distinctive diurnal air temperature variations. Measurement points with less than a total of 10 observations were removed. After data selection and preprocessing, data from 15 days remained for further analyses (Tab. 1).

To ensure comparability in time for measurements from different points, the measured temperature data were converted into differences relative to data observed simultaneously by the reference weather station (WS) Aachen-Hörn (measuring interval=10 min). WS Aachen-Hörn is operated by the Department of Geography at RWTH Aachen University. The station (50°47'N, 06°04'E, 198 m a.s.l.) is situated in a suburban setting with residential and university buildings approximately 1.5 km west of the intersection of the bus routes in the city centre of Aachen (Fig. 1, left).

The radiant surface temperatures were obtained from airborne thermal infrared scanner measurements made for an urban climate analysis on 23 September 1998 between 8 p.m. CEST and 9.30 p.m. CEST (Havlik et al. 2000).

3.2 Land cover and building use

Information on land cover and building use was provided by Aachen's land registry office (KATASTERAMT DER STÄDTEREGION AACHEN 2010) and was used in combination with information on surface sealing (Kopecky and Kahabka 2009) and building height (BEZIRKSREGIERUNG KÖLN 2010). These data were transformed into a new land use classification with a spatial resolution of 2 m based on the classification by Merbitz et al. (2012a). Ten classes were defined, of which 3 classes indicate the degree of surface sealing (10–50%, 50–

Tab. 1: Measuring days with corresponding meteorological conditions (data obtained from the weather station Aachen-Hörn and *DWD)

Date	T_{mean} [°C]	T_{max} [°C]	T_{min} [°C]	T_{amp} [K]	Cloudiness* [okta]	Sunshine duration [h]	Precipitation [mm]	Relative humidity [%]	Wind velocity [Bft]
05.05.2010	8.1	11.9	1.9	10.0	5.6	10.0	0	68	3
21.06.2010	13.9	20.1	8.3	11.8	5.4	8.5	0	65	2
23.06.2010	20.3	25.5	10.3	15.2	1.7	14.2	0	52	1
25.06.2010	21.2	26.6	14.6	12.0	3.5	12.8	0	56	1
30.06.2010	22.9	28.7	15.5	13.2	4.7	13.5	0	57	2
02.07.2010	29.8	35.2	22.0	13.2	5.9	14.3	0	25	2
13.09.2010	14.1	18.3	10.6	7.7	5.3	9.2	0	80	3
17.09.2010	10.9	15.8	8.0	7.8	5.1	5.5	0.4	84	2
20.09.2010	15.5	19.5	11.7	7.8	4.8	9.0	0	65	3
22.09.2010	17.1	24.0	9.5	14.5	1.9	11.2	0	74	2
23.05.2011	17.5	22.7	8.9	13.8	0.3	13.5	0	53	3
25.05.2011	18.2	23.8	5.2	18.6	0.3	14.3	0	34	1
27.05.2011	11.9	16.4	8.7	7.7	6.7	1.0	0	79	3
27.06.2011	26.8	33.6	16.6	17.0	0.4	14.7	0	55	2
28.06.2011	26.8	34.7	20.7	14.0	2.6	11.3	0	58	1

90% and > 90%), 5 classes represent unsealed land (green spaces, forest, water, agriculture and dump sites), and 2 classes classify buildings (residential and industrial) for the whole city area (Fig. 1, right). Altitude differences of up to 285 m required the inclusion of a digital elevation model (DEM). As the vertical temperature gradient was expected to differ strongly in the course of the day, in contrast to Bottyán and Unger (2003), altitude was included as a parameter in the multiple regression analysis based on the ASTER DEM (NASA et al. 2009). The vertical change in air temperature was calculated for the day and evening separately in order to consider atmospheric conditions in an appropriate way.

3.3 Data processing

We performed a multiple regression analysis with observed air temperature data and described altitude and land use parameters (see also Alcoforado and Andrade 2006; Szymanowski and Kryza 2009, 2012) (see chapters 3.1 and 3.2), in which their proportions were considered within radii of 50 m, 100 m, 250 m, 500 m and 1000 m–following the approaches by Ketzler (1997) and Merbitz et al. (2012a, 2012b). The best fits were integrated into a GIS-based model, which allows the calculation of the air temperature differences relative to the reference weather station for the whole city area with a spatial resolution of 10 m in order to illustrate the air temperature distribution for the whole city area. As Svensson et al. (2002) also stated, the main advantage of such a small scale model is the high resolution, which is suitable for use by urban planners.

First, the data were split into an afternoon situation (1 p.m. CET–5 p.m. CET) and an evening situation (8 p.m. CET–12 p.m. CET) to detect possible differences in the magnitude of the influence of the determining factors depending on the time of the day. The time spans of 1 p.m.–5 p.m. and 8 p.m.–12 p.m. were chosen for three reasons. First, the data

set for these two phases had to yield a usable amount of measurements. Secondly, daily intervals of the same lengths (4 hours each) had to be compared. Thirdly, these 4 hours include I) the hottest period of the day and II) in most cases the sunset period. Although the sun set at some days after 8 p.m. the applied time frame was assumed to be reasonable for the evening situation since the cooling phase clearly started before sunset.

4   Results

4. 1 Regression analysis

For the afternoon, 223 measuring points met the criteria of data selection (see chapter 3.1). The measurements during the evening provide fewer data (134 measuring points) because the buses stopped running in some cases before 8 p.m. Furthermore, the measurements in the evening do not include some of the southern parts of Aachen with green spaces and a less dense building structure. As a result, the thermal pattern for the evening situation is not represented as well as the one for the afternoon situation. For the afternoon situation, the step-wise regression yielded the best fit equation when entering green spaces and forest (both 500 m radius), areas of more than 90% sealed surface (250 m radius) and altitude into a multiple regression model (Tab. 2). The multiple R^2 results from the input sequence of the parameters and is updated and accordingly improved with every parameter added to the analysis. For the evening, another composition of determining factors arises (Tab. 3). As the influence of surface sealing decreases, building density gains influence. As some of the land use data were only available within the area of Aachen, some GIS procedures, such as neighborhood statistics, made it necessary to downsize the city limits by a buffer size of 500 m to remove errors that result when examining areas beyond the city limits. Comparing the

Tab. 2: Regression model parameters for air temperature (afternoon)

Input sequence	Parameter (radius)	Coeff.	Single R²	Multiple R²	RMSE
1	Altitude (A)	0.0123915	0.79 (-)		
2	> 90% Sealing (250 m) (S90)	$4.18342e^{-4}$	0.51 (+)		
3	Green spaces (500 m) (G)	$8.0176e^{-5}$	0.46 (-)		
4	Forest (500 m) (F)	$4.3349e^{-5}$	0.21 (-)		
				0.82	0.38

Best fit equation (p < 0.05):
$T = 2.29393 - 0.0123915 * A + 4.18342e^{-4} * S90_{250} - 8.0176e^{-5} * G_{500} - 4.3349e^{-5} * F_{500}$

Tab. 3: Regression model parameters for air temperature (evening)

Input sequence	Parameter (radius)	Coeff.	Single R²	Multiple R²	RMSE
1	Buildings (500 m) (B)	$3.67743e^{-4}$	0.73 (+)		
2	Altitude (A)	0.00447877	0.61 (-)		
3	Forest (500 m) (F)	$1.17895e^{-4}$	0.35 (-)		
				0.80	0.35

Best fit equation ($p < 0.05$):

$T=2.7625+3.67743e^{-4}*B_{500}-0.00447877*A-1.17895e^{-4}*F_{500}$

model results with observed air temperature data the explained variance in both cases (afternoon and evening) exceeds 80% with statistical significance ($\alpha < 0.05$) (Fig. 2). The fact that figure 2 (right) only shows positive temperature differences relative to the suburban reference station may be due to the fragmentary measurements in suburban areas that are colder than the reference station. This may be the reason why a significant correlation between measured air temperature and green spaces was not obtained. Consequently, green spaces were not considered within the multiple regression for the evening situation.

The autocorrelation of the residuals was calculated by Morans I (Li et al. 2007) showing no significant autocorrelation for the midday situation (Morans I=0.24). For the evening situation Morans I is 0.55 supposing clustered values. This can be explained by the lack of measurements in the southern part of Aachen.

The issue of collinearity was addressed by linearly correlating the parameters used in the regression model (Tab. 4). Correlation coefficients were calculated for each pair of the 5 predictors. Except for the correlation between green spaces and forest (p-value=0.77) the partial correlation coefficients are statistically significant at the 95% level of significance (p-value < 0.05).

Although the predictors are not independent of each other, the explained variance of the overall statistical model significantly increases when not only one parameter is included within the regression analysis. Therefore, all parameters are taken into account as they represent different effects of urban structures on air temperature. For example, within urban areas a large percentage of areas without buildings are sealed surfaces without any vegetation, so that building density cannot simply be considered as the residual after subtracting green spaces from an area and vice versa.

The model was cross-validated by sub-dividing the dataset of measured air temperatures into two samples. The parameters of the regression model were calibrated using one sample. The resulting model was evaluated using the other sample by compar-
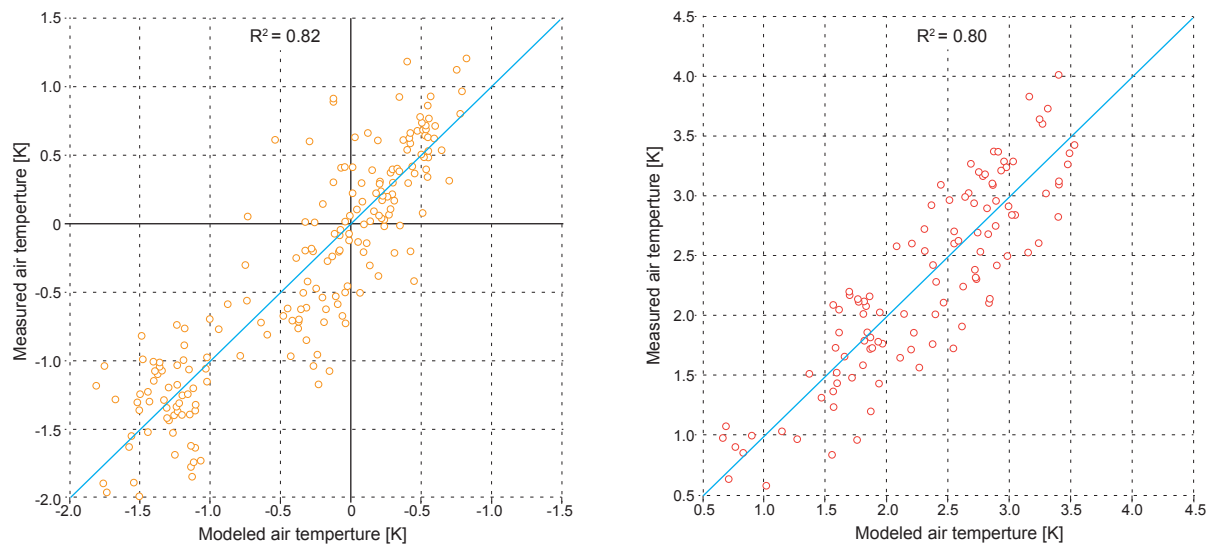

Fig. 2: Comparison of modeled and measured air temperature deviations relative to the reference station [K]; left: afternoon situation, right: evening situation

Tab. 4: Correlation coefficients for each pair of the five predictors used in the regression analysis

	Building density (500 m)	> 90% Sealing (250 m)	Green spaces (500 m)	Forest (500 m)
> 90% Sealing (250 m)	0.58			
Green spaces (500 m)	0.43	0.29		
Forest (500 m)	0.16	0.15	0.00	
Altitude (point value)	0.42	0.36	0.40	0.23

ing the model result to the measured air temperature values of this sample. For the afternoon situation the RMSE is 0.44 (R²=0.71) and 0.36 (R²=0.80). For the evening situation the RMSE is 0.51 (R²=0.63) and 0.47 (R²=0.69) respectively, clearly indicating the reliability of the modelling approach.

Figure 3 illustrates modeled temperature patterns in the city of Aachen. Percentiles indicate the lowest to highest percentages of air tempera-

ture differences relative to the reference station occurring during the afternoon and evening. The air temperature differences between the coldest and warmest areas, which indicate the UHI intensity, is 2.6 K for the afternoon and 2.8 K for the evening respectively. In the evening, the UHI intensity curve has a concentric shape with some local irregularities, as also observed by BOTTYÁN and UNGER (2003). Green spaces (parks and mead-
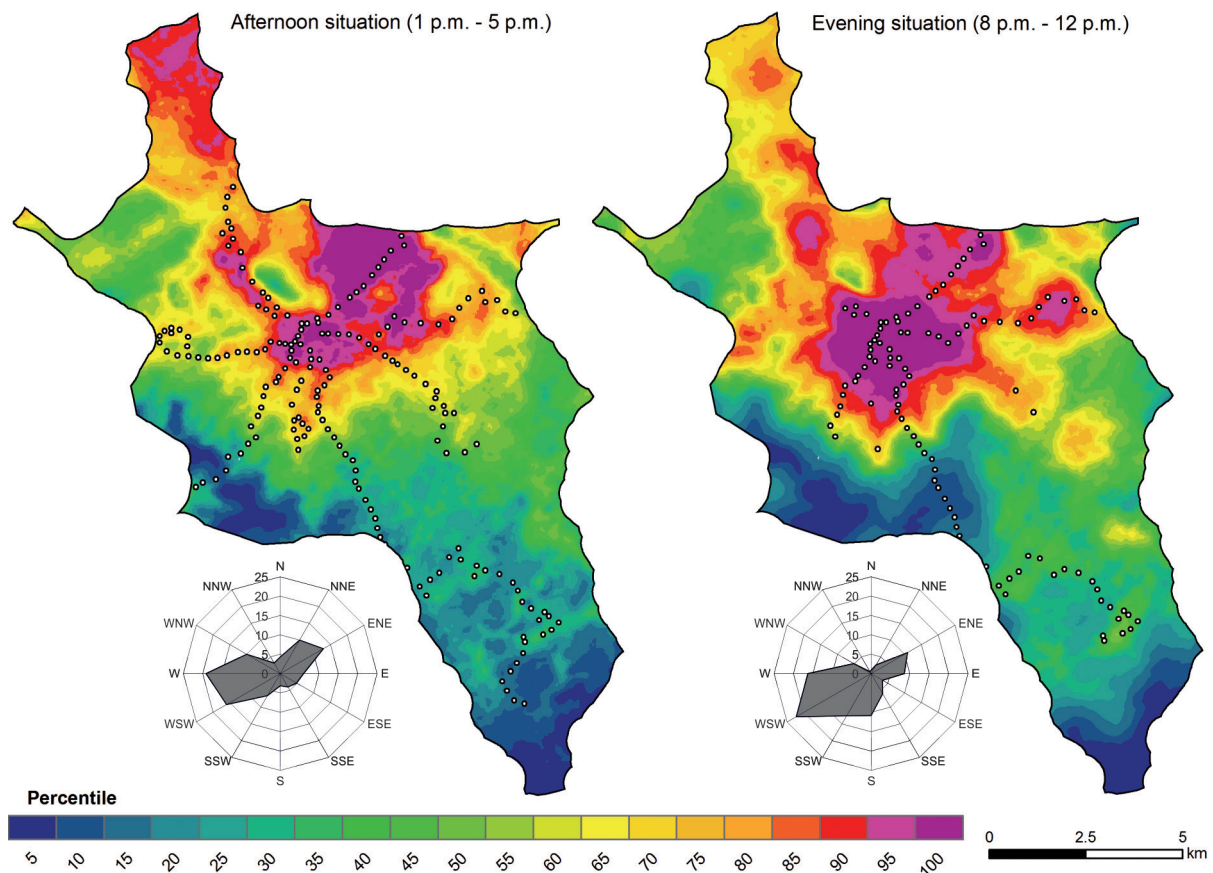

Fig. 3: Modeled air temperature pattern of Aachen for the afternoon (left) and evening (right) with corresponding mean wind directions at WS Aachen-Hörn. The percentiles indicate lowest (blue) to highest (purple) air temperature differences relative to the reference station in 5% steps

ows) and forest sites are the coolest areas, which is mainly due to evaporative cooling and a lack of buildings and surface sealing. Industrial areas northeast of the city centre tend to heat up most intensely during the afternoon. This may be caused by sealed surfaces including parking lots and business parks which are widely exposed to incoming radiation due to a less dense building structure. Different bulk properties and radiative properties of paving materials such as asphalt and building materials contribute to elevated air temperatures. Additionally, there is a relatively large amount of heat release when offices and commercial facilities are in use, as also shown by NARUMI et al. (2009).

The temperature distribution indicates the strong influence of a dense building structure on the air temperature for the evening situation, as is the case for the inner city. Heat is gradually released preventing cooling and keeping air temperatures relatively high. Like many UHI studies, Aachen shows a spatial expansion of the UHI around the inner city core towards the night. Since the model is not able to perceive cold air that originates above green areas and that drains along valleys into the city core, the extent of thermal hot spots may be overestimated at night.

However, it has to be noted that the south of Aachen is only covered by one bus route due to the time schedule of the local bus company. Thus, the measuring network during the evening is less dense compared to the afternoon situation. This may cause biases for the southern and northwestern part of the city for the evening. Since the study focuses on the spatial pattern of the UHI, the relevant areas around the city core are not affected.

An analysis of differences between measured and modeled data was performed to expose the weaknesses of the model. Figure 4 shows an air temperature profile along a route from the southwest to the east of Aachen (Fig. 1, left). While lower air temperatures seem to be generally slightly overestimated, inner-city air temperatures are rather underestimated by the model. One explanation may be that inner urban park sites, which belong to the class of green spaces, do not preponderate within the multiple regression analysis as the buffer size of 500 m captures mostly green spaces outside the inner city. Small sites of urban green are not accounted for significantly. Thus, the sealing degree, which is determined in a buffer of 250 m, has a higher influence within the calculation and, hence, contributes to an overestimation. Further, as the model is not able to consider wind direction, the air temperature for those measuring points next to green spaces on the windward side may be overestimated. The prevailing wind direction for the afternoon is west, for the evening southwest. This may explain the overestimation at the beginning of the profile as the measuring points in the southwest of Aachen are environed by green spaces and forest on the windward side. Inner city and industrial areas produce an urban plume that is advected downwind (OKE 1982) to the north and northeast, resulting in an underestimation of modeled air temperatures north and northeast of the inner city and industrial areas. Although the urban plume is considered rather as a property of the urban boundary layer, this may be a good example of how the UHI structure can be eroded or moved due to local winds. Additionally, heat release from combustion activities promotes elevated temperatures par-
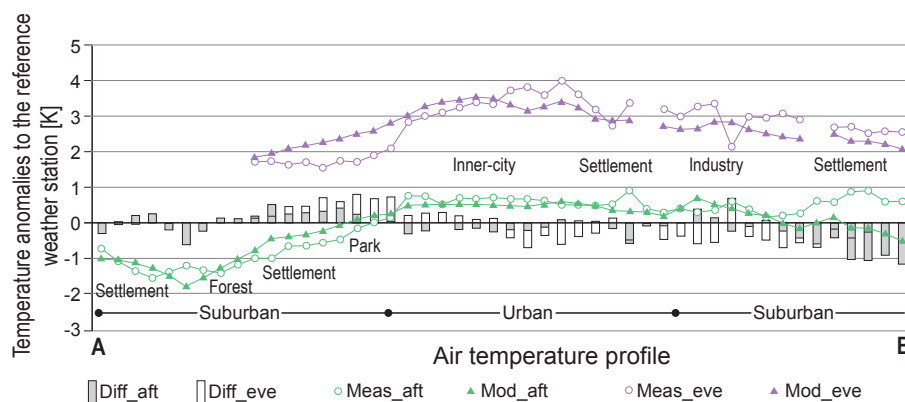

Fig. 4: Measured (Meas) and modeled (Mod) air temperature differences relative to the reference weather station for a profile along one bus route from the southwest to the east of Aachen (Fig. 1, left). Modeled data are illustrated as triangles, measured data as circles (lilac: evening (eve), green: afternoon (aft)). Columns indicate discrepancies (Diff) between observed and modeled data for the afternoon (grey) and evening (white). They are plotted one upon the other to allow a direct comparison between the afternoon and evening situation

ticularly in industrial areas. Discrepancies between measured and modeled data are more pronounced during the evening when cold air drainage flows cool down regions around the inner city.

4.2 Comparison between air temperature and surface temperature pattern

For comparison with surface radiant temperatures, the pixel values of the modeled urban temperature differences for the evening are scaled so that the range matches the temperature values of the thermal imagery. The subtraction of adjusted air temperature values from surface temperatures reveals a map of differences between both measurement methods (Fig. 5, right).

The map of surface radiant temperatures (Fig. 5, left) shows–similar to the distribution of air temperatures–increasing temperatures towards the inner city for an evening situation. Differences are concentrated on forests, streets, topographic depressions (green circles), inner-city core (orange circle) and metal roofs (grey circles). Thermal conductivity, heat capaci-

ty and thermal admittance are the main reasons for the marked temperature differences between densely built-up areas and areas covered mainly by vegetation (Parlow 2003; Nichol et al. 2009). Considering data with a difference of more than 0.5 K between modeled and measured values, more than 90% of these differences are forested areas (Tab. 5). In this case, the surface radiant image is not able to represent the air temperature 2 m above the ground realistically for forests. About one third of modeled air temperatures corresponding to streets are also underestimated due to slow heat release as a function of the high thermal inertia of asphalt paved streets (Buyantuyev and Wu 2010). Other positive deviations between model and remote sensing data are mainly restricted to areas of cold air accumulation during the evening and night, to the densely built-up inner city centre and to buildings with metal roofs, which have low emission values (usually between 0.1 and 0.3 (Stull 2000)) that make them appear too cold.

The latter source of errors occurs–even though to a smaller degree–to roofs in general as they are usually constructed of materials which absorb solar radiation but have low thermal inertia to minimize conductive
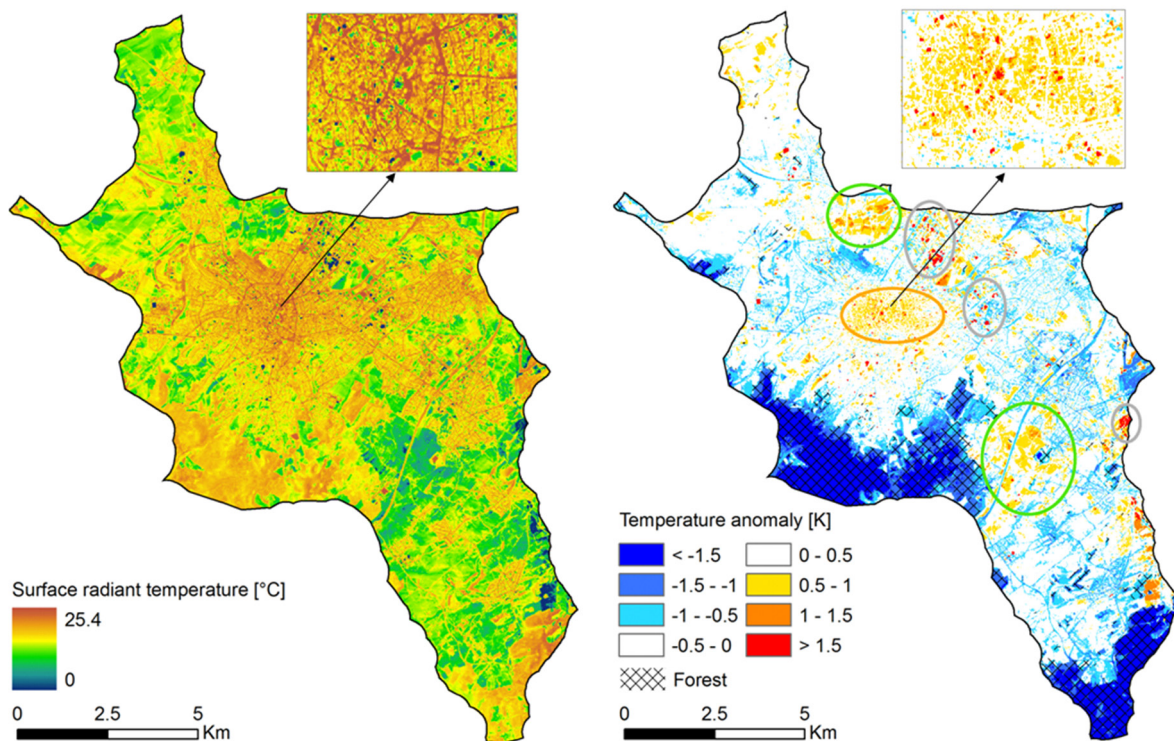

Fig. 5: Left: Thermal image of the city of Aachen (23 September 1998, 8:00–9:20 p.m., scanner type Daedalus AADS 1250, for detailed information see Havlik et al. (2000)). Right: Temperature differences between modeled air temperature values (T_M) and surface radiant temperatures (T_S) ($\Delta T = T_M - T_S$). Circles indicate exemplary areas of temperature deviations (Orange: dense inner city, green: accumulation of cold air, grey: metal roofs)

Tab. 5: Percentage of the temperature differences between modeled air temperature and surface radiant temperatures. Considered are all pixels belonging to the streets, buildings, green or forest variables

Deviations in K	Streets	Buildings	Green	Forest
< -1	7.0	2.2	3.5	79.8
-1 to -0.5	27.3	14.1	12.9	12.8
-0.5 to 0.5	60.3	68.7	71.2	7.0
0.5 to 1	4.3	10.9	10.4	0.3
> 1	1.1	4.1	2.0	0.1

heat transfer (Roth et al. 1989). If the aforementioned deviations are neglected, the modeled air temperature values and surface radiant temperatures match within a range of -0.5 to +0.5 K temperature differences. The fact that surface radiant temperatures and air temperatures are not correlated perfectly can be attributed to the different physics determining the heat exchange. While surface temperatures depend on the surface energy balance, air temperatures are controlled by horizontal and vertical heat fluxes in an air volume (Roth et al. 1989).

5 Discussion

Mobile air temperature measurements using public transport buses provide a comprehensive data set which can be used for various areas of urban climate research. Continuous and simultaneous recordings along 4 routes through the city of Aachen supply a high spatial and temporal resolution. Large sections of the urban area are covered and air temperatures can be recorded during the whole day without any additional costs or time. This is a promising approach that can easily be implemented in agglomerations which offer the necessary infrastructure. For the city of Hamburg the presented approach has already been adopted (Bechtel et al. 2012).

An analysis of air temperature patterns in the city of Aachen based on 15 days and up to 223 measuring points yields specific information on the afternoon at the time of the temperature maximum and on the evening cooling phase.

The thermal conditions are influenced by terrain height and factors in the urban structure such as building density, sealing degree, forest and green spaces. The magnitude of these influences differs according to the period of the day and surface properties. Significant correlations between these urban parameters and air temperature could be determined by means of a multiple linear regression analysis based on observed air temperature data and a land use classification. Despite the fact that air temperature distribution in Aachen is largely determined by terrain, it was possible to make land use and urban structures apparent in the model result. The sky-view-factor (SVF) which describes the urban canyon relates to variables such as building density and building height. Since the incorporation of building height did not contribute to the best fit regarding the multiple regression analysis, this parameter was not further considered within the model setup. In addition, SVF is either related to, or directly derived from, land use factors that are already used in this study. Therefore, the inclusion of the SVF in the multiple regression is not suggested to further improve the model results.

A regression model was applied instead of a kriging model because outside the bus routes additional data such as the proportion of green areas, sealed surfaces or buildings are essential for a robust and plausible model taking land use and surface structure into account. Further, the kriging results only hold for the space between the specified measuring points whereas the applied regression model calculates air temperature values for the whole city area. To fully account for the problem of the partial collinearity between predictors principal component analysis (Vicente-Serrano et al. 2005; Abdi and Williams 2010) could be an alternative in order to deal with inter-correlated variables. By these means the problem of similarity between predictors could be addressed in a further study. "Loadings" of principal components could then be used instead of coefficients relating to original predictors.

With the applied model a high degree of surface sealing accounts for the development of an UHI during the afternoon within the industrial area northeast of the inner city. However, during the evening a high building density has a more significant effect on thermal load. Thus, the UHI shifts in the course of the day from areas beyond the limits of the inner city to the city core. The intra city temperature differenc-

es are 2.6 K during the afternoon and slightly higher (2.8 K) during the evening.

The presented model does not take wind direction into account. Thus, advection is neglected and temperature in downwind areas may be underestimated. As wind direction may modify the UHI (VICENTE-SERRANO et al. 2005) this parameter needs to be added for further improvement of the model. Since the relationship between temperature and land use factors is not constant over space, a local regression model, e.g. geographically weighted regression with adaptive kernels, may be an option to tackle all peculiarities and non-stationary processes within the region of Aachen. This approach would only be reasonable if enough data could be surveyed on a local scale. Furthermore, this approach may worsen the transferability of the model approach to other urban areas. However, the comparison between modeled and measured air temperatures shows an explained variance of 0.80 (afternoon) and 0.82 (evening) respectively, indicating that the model results are not strongly violated by this effect.

A comparison with thermal imagery of surface radiant temperatures for the evening situation is in good accordance with modeled air temperatures except for those areas where energy exchange processes differ strongly between the surface and ambient air at 2 m above the ground. This is the case for forested areas where surface temperature relates to canopies much higher than 2 m above the ground, buildings with roofs characterized by a low emissivity coefficient, and cold air accumulation sites. Although surface temperatures can be significantly different from ambient air temperatures due to turbulence and velocity activities in the ambient air mass (MIRZAEI and HAGHIGHAT 2010), most of the remaining areas show deviations in surface radiant temperatures in a range of less than -0.5 K to +0.5 K. Air temperatures at ground level and surface temperatures at roof level are obviously different. Nevertheless, it was surprising that both parameters yielded such a good accordance. This supports the idea that surface temperature also delivers useful information regarding patterns of air temperature. Taking a wider environment into account to describe the relationship between surface and air temperature, the influence of the nearby surface temperatures on the air temperature at a given point may even refine the results (UNGER et al. 2010).

Since the UHI can be used as one parameter to consider heat exposure for urban residents, future studies must aim at relating environmental stressors to social attributes. For these issues, descriptive statistics of the diurnal and spatial air temperature evolution in the city of Aachen with special regard to the variances and extremes would need to be applied.

References

ABDI, H. and WILLIAMS, L. J. (2010): Principal component analysis. In: Computational Statistics 2 (4), 433–459. DOI: 10.1002/wics.101

ALCOFORADO, M.-J. and ANDRADE, H. (2006): Nocturnal urban heat island in Lisbon (Portugal): main features and modelling attempts. In: Theoretical and Applied Climatology 84, 151–159. DOI: 10.1007/s00704-005-0152-1

ARNFIELD, A. J. (2003): Two decades of urban climate research: a review of turbulence, exchanges of energy and water, and the urban heat island. In: International Journal of Climatology 23, 1–26. DOI: 10.1002/joc.859

BÄRRING, L. and MATTSSON, J. O. (1985): Canyon geometry, street temperatures and urban heat island in Malmö, Sweden. In: Journal of Climatology 5, 433–444. DOI: 10.1002/joc.3370050410

BBSR (BUNDESINSTITUT FÜR BAU-, STADT- UND RAUMFORSCHUNG) (ed.) (2011): Zurück in die Stadt. BBSR-Berichte KOMPAKT 2, 1–19.

BECHTEL, B.; LANGKAMP, T.; BÖHNER, J.; DANEKE, C.; OSSEN-BRÜGGE, J. and SCHEMPP, S. (2012): Classification and modelling of urban micro-climates using multisensoral and multitemporal remote sensing data. XXXIX-B8. XXII ISPRS Congress, 25 August–01 September 2012, Melbourne, Australia.

BEZIRKSREGIERUNG KÖLN (2010): Geobasis NRW. Produkte und Dienste 2010/2011.

BOTTYÁN, Z. and UNGER, J. (2003): A multiple linear statistical model for estimating the mean maximum urban heat island. In: Theoretical and applied Climatology 75, 233–243. DOI: 10.1007/s00704-003-0735-7

BRÜCKER (2005): Vulnerable populations: lessons learnt from the summer 2003 heat waves in Europe. In: Euro-surveillance 10 (7–9), 147.

BRUSE, M. (2003): Stadtgrün und Stadtklima. In: LÖBF-Mitteilungen 1, 66–70.

BUTTSTÄDT, M.; SACHSEN, T.; KETZLER, G.; MERBITZ, H. and SCHNEIDER, C. (2011): A new approach for highly resolved air temperature measurements in urban areas. In: Atmospheric Measurement Techniques Discussion 4, 1001–1019.

BUYANTUYEV, A. and WU, J. (2010): Urban heat islands and landscape heterogeneity: linking spatiotemporal variations in surface temperatures to land-cover and socioeconomic patterns. In: Landscape Ecology 25, 17–33. DOI: 10.1007/s10980-009-9402-4

DOBLER, G. and JENDRITZKY, G. (2001): Diseases and climate. In: LOZÁN, J. L.; GRASSL, H.; and HUPFER, P. (eds.): Climate of the 21st century: changes and risks. Hamburg, 331–337.

ELIASSON, I. (1992): Infrared thermography and urban temperature patterns. In: International Journal of Remote Sensing 13 (5), 869–879. DOI: 10.1080/01431169208904160

EUROPEAN COMMISSION (2010): Demography Report. Older, more numerous and diverse Europeans. Luxembourg.

GABRIEL, K. M. A. and ENDLICHER, W. R. (2011): Urban and rural mortality rates during heat waves in Berlin and Brandenburg, Germany. In: Environmental Pollution, 1–7. DOI: 10.1016/j.envpol.2011.01.016

GRUNDY, E. (2006): Ageing and vulnerable elderly people: European perspectives. In: Ageing & Society 26, 105–134. DOI: 10.1017/S0144686X05004484

HARLAN, S. L.; BRAZEL, A. J.; PRASHAD, L.; STEFANOV, W. I. L. and LARSEN, L. (2006): Neighborhood microclimates and vulnerability to heat stress. In: Social Science & Medicine 63 (11), 2847–2863. DOI: 10.1016/j.socscimed.2006.07.030

HAVENITH, G. (2005): Temperature regulation, heat balance and climatic stress. In: KIRCH, W.; MENNE, B. and BERTOLLINI, R. (eds.): Extreme weather events and public health responses. Berlin, Heidelberg, New York, 69–80.

HAVLIK, D. and KETZLER, G. (2000): Gesamtstädtisches Klimagutachten Aachen. Aachen.

HAVLIK, D.; KETZLER, G.; PESCHEL, G. and STEINICKE, W. (2000): Thermalkarte Aachen. In: Informationen und Materialien zur Geographie der Euregio Maas-Rhein 47, 21–34.

HEISLER, G. M. and BRAZEL, A. J. (2010): The urban physical environment: temperature and urban heat islands. In: AITKEN-HEAD-PETERSON, J. and VOLDER, A. (eds.): Urban Ecosystem Ecology. Madison, 29–56.

HEUSINKVELD, B. G.; VAN HOVE, L. W. A.; JACOBS, C. M. J.; STEENEVELD, G. J.; ELBERS, J. A.; MOORS, E. J. and HOLTSLAG, A. A. M. (2010): Use of a mobile platform for assessing urban heat stress in Rotterdam. Proceedings of the 7th Conference on Biometeorology. Freiburg, 433–438.

HJORT, J.; SUOMI, J. and KÄYHKÖ, J. (2011): Spatial prediction of urban-rural temperatures using statistical methods. In: Theoretical and Applied Climatology 106, 139–152. DOI: 10.1007/s00704-011-0425-9

HUYNEN, M. M. T. E.; MARTENS, P.; SCHRAM, D.; WEIJENBERG, M. P. and KUNST, E. A. (2001): The impact of heat waves and cold spells on mortality rates in the Dutch population. In: Environmental Health Perspectives 109 (5), 463–470. DOI: 10.1289/ehp.01109463

KATASTERAMT DER STÄDTEREGION AACHEN (2010): Geobasisdaten aus dem Liegenschaftskataster.

KETZLER, G. (1997): Vergleichende Untersuchungen der Temperaturverhältnisse in Städten unter besonderer Berücksichtigung der Temperaturänderungsraten. Aachener Geographische Arbeiten 31. Aachen.

KLYSIK, K. and FORTUNIAK, K. (1999): Temporal and spatial characteristics of the urban heat island of Lodz, Poland. In: Atmospheric Environment 33, 3885–3895. DOI: 10.1016/S1352-2310(99)00131-4

KOPECKY M. and KAHABKA H. (2009): EEA-FTSP-Sealing-Enhancement Updated Delivery Report European Mosaic. European Environment Agency Report.

KUTTLER, W. (2001): Urban climate and global climate change. In: LOZÁN, J. L.; GRASSL, H. and HUPFER, P. (eds.): Climate of the 21st century: changes and risks. Hamburg, 344–350.

LANDSBERG (1970): Man-made climatic changes. In: Science 170, 1265–1274. DOI: 10.1126/science.170.3964.1265

LEE, D. O. (1984): Urban climates. In: Progress in Physical Geography 8 (1), 1–31. DOI: 10.1177/030913338400800101

LI, H.; CALDER, C. A. and CRESSIE, N. (2007): "Beyond Moran's I: Testing for spatial dependence based on the spatial autoregressive model". In: Geographical Analysis 39 (4), 357–375. DOI: 10.1111/j.1538-4632.2007.00708.x

LO, C. P.; QUATTROCHI, D. A. and LUVALL, J. C. (1997): Application of high-resolution thermal infrared remote sensing and GIS to assess the urban heat island effect. In: International Journal of Remote Sensing 18 (2), 287–304. DOI: 10.1080/014311697219079

MERBITZ, H.; FRITZ, S. and SCHNEIDER, C. (2012a): Mobile measurements and regression modeling of the spatial particulate matter variability in an urban area. In: Science of the Total Environment 438, 389–403. DOI: 10.1016/j.scitotenv.2012.08.049

MERBITZ, H.; BUTTSTÄDT, M.; MICHAEL, S.; DOTT, W. and SCHNEIDER, C. (2012b): GIS-based identification of spatial variables enhancing heat and poor air quality in urban areas. In: Applied Geography 33 (4), 94–106. DOI: 10.1016/j.apgeog.2011.06.008

MIRZAEI, P. A. and HAGHIGHAT, F. (2010): Approaches to study urban heat island–abilities and limitations. In: Building and Environment 45, 2192–2201. DOI: 10.1016/j.buildenv.2010.04.001

MONTÁVEZ, J. P.; RODRÍGUEZ, A. and JIMÉNEZ, L. J. (2000): A study of the urban heat island of Granada. In: International Journal of Climatology

20,899–911.DOI:10.1002/1097-0088(20000630)20:8<899::AID-JOC433>3.0.CO;2-I

Narumi, D.; Kondo, A. and Shimoda, Y. (2009): Effects of anthropogenic heat release upon the urban climate in a Japanese megacity. In: Environmental Research 109, 421–431. DOI: 10.1016/j.envres.2009.02.013

NASA; METI and USGS (2009): ASTER Global DEM Validation. Summary Report. https://lpdaac.usgs.gov/content/view/full/11033 (15 January 2012).

Nichol, J. E.; Fung, W. F.; Lam, K. and Wong, M. S. (2009): Urban heat island diagnosis using ASTER satellite images and 'in situ' air temperature. In: Atmospheric Research 94, 276–284. DOI: 10.1016/j.atmosres.2009.06.011

Oke, T. R. (1980): Climatic impacts of urbanization. In: Bach, W.; Pankrath, J. and Williams, J. (eds.): Interactions of energy and climate. Boston, 339–356.

– (1982): The energetic basis of the urban heat island. In: Quarterly Journal of the Royal Meteorological Society 108 (455), 1–24. DOI: 10.1002/qj.49710845502

– (1997): Urban climates and global environmental change. In: Thompson, R. D. and Perry, A. (eds.): Applied climatology: principles & practices. New York, 273–287.

– (2001): Boundary layer climates. Cambridge.

Parlow, E. (2003): The urban heat budget derived from satellite data. In: Geographica Helvetica 58 (2), 99–111. DOI: 10.5194/gh-58-99-2003

Pease, R. W.; Lewis, J. E. and Outcalt, S. I. (1976): Urban terrain climatology and remote sensing. In: Annals of the Association of American Geographers 66 (4), 557–569. DOI: 10.1111/j.1467-8306.1976.tb01110.x

Rosenzweig, C.; Solecki, W. D.; Parshall, L.; Chopping, M.; Pope, G. and Goldberg, R. (2005): Characterizing the urban heat island in current and future climates in New Jersey. In: Environmental Hazards 6 (1), 51–62. DOI: 10.1016/j.hazards.2004.12.001

Roth, M.; Oke, T. R. and Emery, W. J. (1989): Satellite-derived urban heat islands from three coastal cities and the utilization of such data in urban climatology. In: International Journal of Remote Sensing 10 (11), 1699–1720. DOI: 10.1080/01431168908904002

Saito, I.; Ishihara, O. and Katayama, T. (1990/91): Study of the effect of green areas on the thermal environment in an urban area. In: Energy and Buildings 15 (3–4), 493–498. DOI: 10.1016/0378-7788(90)90026-F

STADT AACHEN (2009): Sozialentwicklungsplan Aachen. Aachen.

Straka, J. M.; Rasmussen, E. N. and Fredrickson, S. E. (1996): A mobile mesonet for finescale meteorological observations. In: Journal of Atmospheric and Oceanic Technology 13 (5), 921–936. DOI: 10.1175/1520-0426(1996)013<0921:AMMFFM>2.0.CO;2

Stull, R. B. (2000): Meteorology for scientists and engineers. Pacific Grove, CA.

Svensson, M. K.; Eliasson, I. and Holmer, B. (2002): A GIS based empirical model to simulate air temperature variations in the Göteborg urban area during the night. In: Climate Research 22, 215–226. DOI: 10.3354/cr022215

Szymanowski, M. and Kryza, M. (2009): GIS-based techniques for urban heat island spatialization. In: Climate Research 38, 171–187. DOI: 10.3354/cr00780

– (2012): Local regression models for spatial interpolation of urban heat island–an example from Wroclaw, SW Poland. In: Theoretical and Applied Climatology 108, 53–71. DOI: 10.1007/s00704-011-0517-6

Tayanç, M. and Toros, H. (1997): Urbanization effects on regional climate change in the case of four large cities of Turkey. In: Climatic Change 35, 501–524. DOI: 10.1023/A:1005357915441

Unger, J. (2004): Intra-urban relationship between surface geometry and urban heat island: review and new approach. In: Climate Research 27, 253–264. DOI: 10.3354/cr027253

Unger, J.; Sümeghy, Z.; Gulyás, Á.; Bottyán, Z. and Mucsi, L. (2001): Land-use and meteorological aspects of the urban heat island. In: Meteorological Applications 8, 189–194. DOI: 10.1017/S1350482701002067

Unger, J.; Gál, T.; Rakonczai, J.; Mucsi, L.; Szatmári, J.; Tobak, Z.; Van Leeuwen, B. and Fiala, K. (2010): Modeling of the urban heat island pattern based on the relationship between surface and air temperatures. In: Időjárás 114 (4), 287–302.

Vicente-Serrano, S. M.; Cuadrat-Prats, J. M. and Saz-Sánchez, M. A. (2005): Spatial patterns of the urban heat island in Zaragoza (Spain). In: Climate Research 30, 61–69. DOI: 10.3354/cr030061

Yamashita, S. (1996): Detailed structure of heat island phenomena from moving observations from electric tram-cars in Metropolitan Tokyo. In: Atmospheric Environment 33 (3), 429–435. DOI: 10.1016/1352-2310(95)00010-0

Authors

Mareike Buttstädt, M.A.
RWTH Aachen University
Human Technology Centre, "City 2020+"
Theaterplatz 14
52056 Aachen
Germany
mareike.buttstaedt@geo.rwth-aachen.de

Prof. Dr. Christoph Schneider
RWTH Aachen University
Department of Geography
Wüllnerstraße 5b
52062 Aachen
Germany
christoph.schneider@geo.rwth-aachen.de